An Effect of Explosive Detonation Pressures on Fragmentation Characteristics of Explosive Fragmentation Munitions

V.M. Gold and Y. Wu
U.S. Army RDECOM-ARDEC, Attn: AMSRD-AAR-AEE-W, Bldg. 3022
Picatinny Arsenal, NJ 07806, USA
e-mail: vladimir.gold@us.army.mil

1. Abstract.

A study of the effect of high explosive composition formulations on fragmentation characteristics of naturally fragmenting explosive fragmentation munitions had been conducted. The assessment of the fragment mass distribution of tested charges was accomplished using arena test and sawdust fragment recovery experimentation. The analytical assessment of the fragmentation parameters was performed employing the PAFRAG (Picatinny Arsenal Fragmentation) modeling methodology which links three-dimensional axial symmetric high-strain high-strain-rate hydrocode analyses with a phenomenological fragmentation model based on the Mott's theory of break-up of ideal cylindrical "ring-bombs". The studied high explosive compositions included a series of formulations with varying Chapman-Jouguet detonation pressure levels. The fragment mass distribution parameters had been determined to be a strong function of the detonation properties of the explosives. The PAFRAG modeling analysis has been shown to accurately reproduce available experimental fragmentation data.

2. Introduction.

The influence of high explosive parameters on fragmentation characteristic of explosive fragmentation munitions has long been of interest in the military field and has recently commanded considerable attention in the support Insensitive Munition efforts aimed to increase ammunition's safety due to accidental and hostile fires and bullet and fragment impacts. In the Gulf War, for example, most of the disabling damage to fighting vehicles was found to be caused by vehicles own munition payloads, inadvertently triggered by the unwanted stimuli.

3. PAFRAG-Mott Fragmentation Modeling.

A study of the effect of explosive detonation pressures on fragmentation characteristics of explosive fragmentation munitions presented in this work was performed employing the PAFRAG (Picatinny Arsenal Fragmentation) modeling methodology [1] which links three-dimensional axial symmetric high-strain high-strain-rate CALE [2] hydrocode analyses with a semi-empirical fragmentation model PAFRAG-Mott [3]. CALE is a plane two-dimensional and three-

dimensional axial symmetric high rate finite difference computer program [2] based on Arbitrary Lagrangian-Eulerian formulation of the governing equations.

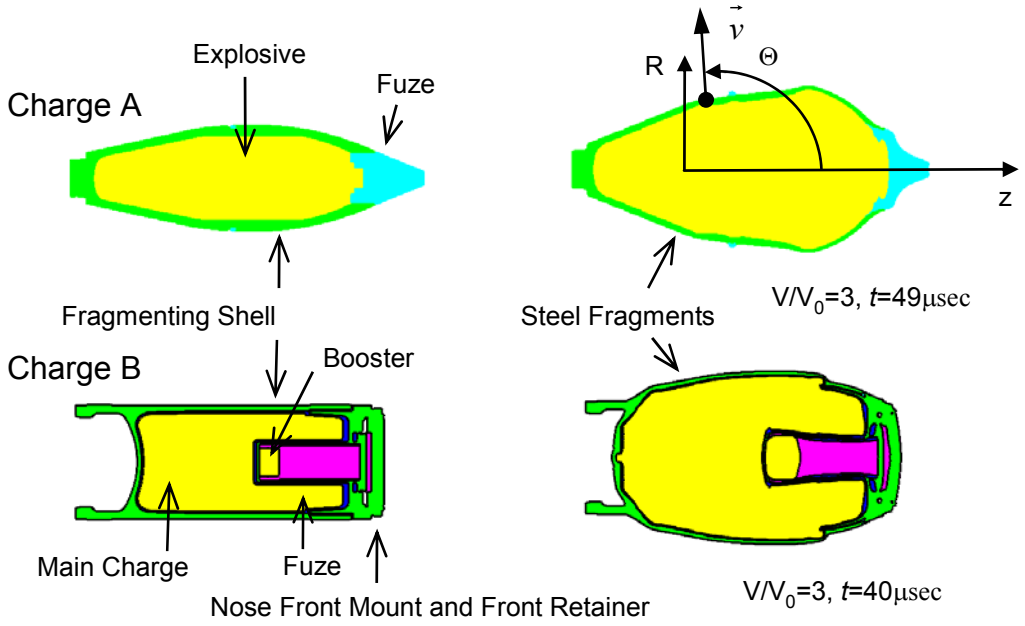

Fig. 1 Results of CALE-code modeling: initial configuration and CALE's predictions following the explosive detonation initiation.

The geometries of two example problems considered in this work are shown in Fig. 1. Upon initiation of the high explosive charges, rapid expansion of high pressure high-velocity detonation products results in high-strain high-strain-rate dilation of the hardened steel shells, which eventually rupture generating a "spray" of high-velocity steel fragments. Defining the longitudinal axis of the munition as the polar axis *z*, the resulting flight trajectories of the fragment spray can be referenced using the polar altitudinal angles Θ measured from the munition's nose (Θ=0°) to tail (Θ=180°).

In fragmentation arena tests, the ammunition fragmentation characteristics are assessed as functions of polar angles Θ identifying angular positions of fragment-catching witness panels and velocity-measuring screens. In PAFRAG code analyses, positions of these devices are irrelevant, and the fragmentation characteristics are assessed in reference to the fragment trajectory angles Θ' calculated from the CALE code cell velocities at the time of the shell break-up. Once the shell breaks up and fragments are formed, fragment velocities may change with time due to a number of reasons, including the air drag and the rigid body motion induced at the time of the shell break up. Assuming that the fragment trajectory angles Θ' do not change with time (that is the rigid body motion and the lateral drift of fragments due to air resistance is relatively small) and that the definitions of angles Θ and Θ' are approximately identical, the PAFRAG model enables prediction of crucial characteristics of explosive

fragmenting munitions including the number of fragments, the fragment size distribution, and the average fragment velocities.

The mathematical description of the PAFRAG-Mott code is given here for completeness. For a large part the PAFRAG-Mott code fragmentation model is based on the Mott's theory of break-up of cylindrical "ring-bombs" [4], in which the average length of the resulting circumferential fragments is a function of the radius and velocity of the ring at the moment of break-up, and the mechanical properties of the metal. A comprehensive review of the Motts theory, including the state-of-the-art developments and applications is given by Grady [5]. Following Mott and Linfoot [6], the "random variations" in fragment sizes are accounted through the following fragment distribution relationship

$$N(m) = N_0 e^{-\left(m/\mu\right)^{1/2}} \qquad \textbf{(1)}$$

In equation **(1)** $N(m)$ represents total number of fragments of mass greater than m, μ is defined as one half of the average fragment mass, $N_0=M/\mu$, and M is the total mass of the fragments.

In attempting to evaluate the distribution of fragment sizes occurring in the dynamic fragmentation of expanding metal rings, Mott [4] introduced an idealized model in which the average circumferential fragment lengths are not random but determined by the interaction of stress release waves originating from instantaneous fractures in the body. Thus, according to Mott's theory the average size of fragments is determined by the rate at which stress relieved regions spread through the plastically expanding ring and the average circumferential length of the resulting fragments is

$$x_0 = \left(\frac{2\sigma_F}{\rho\gamma'}\right)^{1/2} \frac{r}{V} \qquad \textbf{(2)}$$

In equation **(2)** ρ and σ_F denote the density and the strength, respectively; r is the radius of the ring, V is the velocity with which the shell is moving outwards, and γ' is a semi-empirical statistical constant determining the dynamic fracture properties of the material.

Given that the rugged-shaped fragments can be idealized with simple geometric shapes such as parallelepipeds [7,8] having longitudinal length l_0, breadth x_0, and thickness t_0, the average fragment mass takes the following form

$$\mu = \frac{1}{2}\alpha\rho x_0^3 \qquad \textbf{(3)}$$

In equation **(3)**, $\alpha = \frac{l_0}{x_0}\cdot\frac{t_0}{x_0}$. Substituting equation **(2)** into equation **(3)** results in

$$\mu = \frac{1}{2}\left(\frac{2\sigma_F}{\rho^{1/3}\alpha^{-2/3}\gamma'}\right)^{3/2}\left(\frac{r}{V}\right)^3 \qquad \textbf{(4)}$$

Since the fragment distribution relationship, equation **(1)**, warrants knowledge of the average fragment mass but not the shape, introducing

$$\gamma = \alpha^{-2/3}\gamma' \tag{5}$$

equation **(4)** can be put in a simpler and more useful form

$$\mu = \frac{1}{2}\left(\frac{2\sigma_F}{\rho^{1/3}\gamma}\right)^{3/2}\left(\frac{r}{V}\right)^3 \tag{8}$$

For computational purposes, in PAFRAG code, the shell is "divided" into a finite number of short "ring" segments, N, each "ring" j corresponding to the respective fragment spray Θ-angle trajectory, Θ_j. For each ring element j uniform field variables are assumed, and the values of the total fragment mass, m_j, the average fragment velocity, V_j, and the shell break-up radius, r_j, are calculated. Accordingly, the PAFRAG-Mott model fragment distribution is defined as

$$N(m) = \sum_j N_{0j} e^{-\left(m/\mu_j\right)^{1/2}} \tag{9}$$

In equation **(9)**, μ_j and N_{0j} denote the one half of the average fragment mass and the total number of fragments projected from the "ring" j at the trajectory angles Θj, respectively. The values of μ_j and N_{0j} are determined through the following relationships:

$$\mu_j = \sqrt{\frac{2}{\rho}}\left(\frac{\sigma_F}{\gamma}\right)^{3/2}\left(\frac{r_j}{V_j}\right)^3 \tag{10}$$

$$N_{0j} = \frac{m_j}{\mu_j} \tag{11}$$

4. PAFRAG Analysis and Experimentation Results.

As an integral part of the study of this work, a set of the prototype "Charge A" warheads loaded with a series of IM (Insensitive Munition) explosive formulations had been fabricated and tested. The brisance properties of the studied compositions had been varied from a "near-ideal detonating" Comp-B (60% RDX, 40% TNT) and HBU-88B (88% RDX, 12% HTPB binder with additives) to a "non-ideal" PAX-25 (60% DNAN with a stabilizing agent, MNA, 20% RDX, 20% AP), fulminating in a wide range of detonation pressures from approximately 29.5 GPa for Comp-B to approximately 17.5 GPa for PAX-25. The fragmentation performance of the explosive compositions studied was assessed employing the Picatinny Arsenal "closed chamber" sawdust fragment recovery technique, or the "pit" test [9] complemented with a series of the PAFRAG analyses. In the case of the "baseline" Comp-B formulation, in addition to the sawdust "pit" test data of this work, the fragmentation arena test records had been also available, offering an opportunity for comparison between two independent sets of fragmentation data.

Fig. 2 shows plots of the cumulative number of fragments versus the fragment mass m for the prototype "Charge A" warheads loaded with the Comp-B, the HBU-88B, and the PAX-25 explosive formulations considered. All analytical

curves shown in the figure had been obtained through "fitting" the PAFRAG-Mott model analyses with the experimental data under an assumption that the fragmentation occurs instantly at approximately 3 volume expansions of detonation products. The curve "fitting" had been accomplished through varying the value of the fracture parameter γ in equation **(10)**, aiming to achieve the best agreement between the analyses and the recovered cumulative number of fragments $N(m)$ for fragments with masses greater than 2 grains, m=2. As shown in the figure, when changing the "baseline" Comp-B explosive fill composition to the HBU-88B and the PAX-25 formulations, the cumulative number of fragments $N(m)$ had decreased by appreciable 9% and 32%, respectively. This is a very interesting result, since from the available cylinder test data the "Comp-B-scaled" HBU-88B and PAX-25 Gurney velocity constants are only modestly smaller then unity by approximately 2% (0.981) and 5% (0.952), respectively.

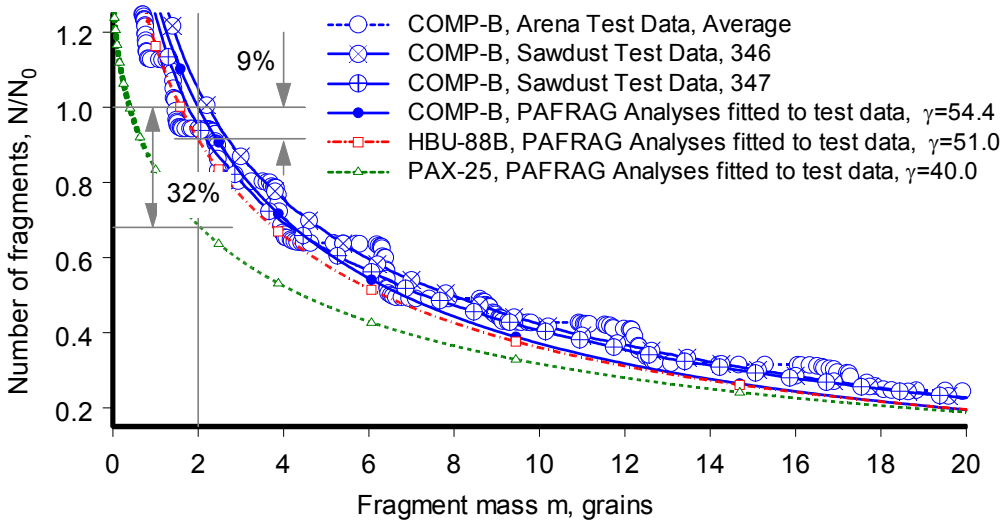

Fig. 2 Cumulative number of fragments versus fragment mass, Charge A. N_0 is the average cumulative number of fragments with mass m greater than 2 grains from all "baseline" Comp-B fragment recovery tests.

To examine parameters affecting performance of fragmentation munitions with changes of the explosives, consider the Mott distribution function, equation **(1)**. Since the lethality of fragmentation warheads is approximately proportional to numbers of fragments generated, denoting explosive compositions by indices "1" and "2", the change of the fragmentation performance is given by the ratio of the total number of fragments:

$$\frac{N_2}{N_1} = \frac{\mu_1}{\mu_2} \qquad \textbf{(12)}$$

In equation **(12)** index "1" denotes the reference baseline, and index "2" implies an arbitrary variation of the baseline munition, such as the HBU-88B, or the PAX-25 explosives fill compositions considered. Substituting equation **(8)** into equation **(12)** and assuming that the fragment shape coefficient α, the flow stress

at fracture σ_F, and the fracture radii r are approximately the same; the ratio of the total number of fragments is given by the equation

$$\frac{N_2}{N_1} = \left(\frac{\gamma_2}{\gamma_1}\right)^{3/2} \left(\frac{V_2}{V_1}\right)^3 \qquad \textbf{(13)}$$

Since the Mott distribution function, equation **(1)**, is a monotonically increasing function of the fragment mass m, equation **(13)** represents the extremum of possible variances of the cumulative number of fragments. Equation **(13)** identifies two major parameters affecting the fragmentation performance of explosive fragmentation munitions: the fragment velocities V and the fracture parameter γ. The fragment velocities V are proportional to the amount of the thermochemical energy released by the detonating explosive when captured and transformed into the mechanical kinetic energy of the dilating metal shell; the values of V are usually well defined empirical functions of the brisance and the density of explosive compositions. According to the to Mott's theory, equation **(2)**, the fragment velocities determine the rate at which stress relieved regions spread through the plastically expanding shell, which defines the average circumferential size and the mass of fragments. Accordingly, as given by equation **(13)**, the total number of fragments is proportional to the velocities in the power of three and, therefore, the munition fragmentation performance is very sensitive to the brisance and the density of the explosive fill composition. The second parameter that defines the fragmentation performance is the fracture parameter γ. A plot of the PAGRAG-Mott calculated values of the fracture parameter γ versus the explosive detonation Chapman-Jouguet (CJ) pressure is shown in Fig. 3.

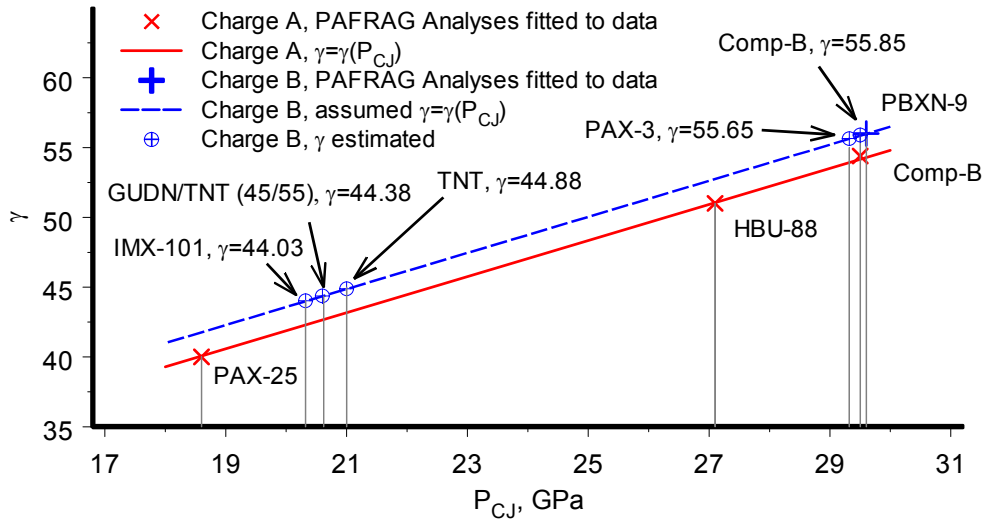

Fig. 3 Parameter γ versus explosive detonation Chapman-Jouguet (CJ) pressure

As shown in the plot, values of γ for the prototype "Charge A" warhead had been obtained through "fitting" the PAFRAG-Mott model analyses with the experimental data, Fig. 2, resulting in an approximately linear relationship between the fracture parameter γ and the explosive detonation Chapman-Jouguet

(CJ) pressures, P_{CJ}. Examining the mathematical form of the "theoretical" values of the parameter γ' is of interest. Following the fundamental assumption of Mott [4] that initiation of fractures in plastically expanding metal shells is due to microscopic flaws and cracks normally present in all metals, the value of the parameter γ' is given by the following relationship

$$\gamma' = 2\ln(\mathcal{N}\mathcal{V})\frac{1}{n}\frac{d(\ln\sigma)}{d\varepsilon} \qquad \textbf{(14)}$$

In equation **(14)** $\mathcal{N}$ represents a number of microscopic flaws in a unit volume $\mathcal{V}$, parameter n is an exponent in the relationship between the stress σ at which the crack spreads and the length of the crack, and ε is the strain. Employing the shear-modulus-pressure-dependent yield strength model of Steinberg and Guinan [10] commonly used for modeling high strain high-strain-rate behavior of metal shells driven by explosives, and assuming that the initial strain in the shell $\varepsilon_i = 0$, and that the shell fractures when the principle strain reaches the value of ε_F, equation **(14)** takes following form

$$\gamma' = 2\ln(\mathcal{N}\mathcal{V})\frac{1}{n}\frac{\delta\beta}{1+\beta\varepsilon_F} \qquad \textbf{(15)}$$

Given that the experimentally observed relationship between the parameter γ and the explosive detonation pressures P_{CJ} is approximately linear, and assuming that the strain hardening parameters δ and β and the shell fracture stain ε_F of equation **(15)** are not affected by the shock wave that drives the shell, it follows then that the shell cumulative damage term $\ln(\mathcal{N}\mathcal{V})$ has also be a linear function of P_{CJ}. The physical meaning of this finding is that the cumulative damage $\ln(\mathcal{N}\mathcal{V})$ sustained from the explosive detonation shock waves traversing through the shell is directly proportional to the "strength" of the "reverberations" of tensile rarefaction pulses opening and coalescing microscopic voids normally present in the shell material, ultimately resulting in increases of the number of microscopic flaws and cracks $\mathcal{N}$ in the shell. Similar results of approximately linear cumulative flaw and crack number distribution functions had been reported by Curran [11] by direct measurements of fracture damages of polished sections of 1145 Aluminum and ARMCO iron specimens from high-velocity plate impact experiments.

Thus, considering two or more explosive fragmentation munitions made from the same grades of steel with similar fabrication and heat treatment processing and schedules, but with different geometries, and assuming that the fragment shape factor α, equation **(5)**, is approximately the same, a generic set of the $\gamma(P_{CJ})$ functions for these warheads can be approximated by a family of straight parallel lines with the same slope defined by the $\ln(\mathcal{N}\mathcal{V})$ term, accounting for to the microstructural properties of the shell material. Accordingly, as shown in Fig. 3, the $\gamma(P_{CJ})$ function for the prototype "Charge B" munition had been defined as a straight line parallel to that of the prototype "Charge A" warhead and passing through a "known" PBXN-9 γ-point. Similar to the prototype "Charge A"

warhead, the value of γ for the baseline "Charge B" PBXN-9 explosive composition had been obtained through "fitting" the PAFRAG-Mott model analyses to the experimental data.

After establishing the $\gamma(P_{CJ})$ relationship, the fragmentation performance of prototype "Charge B" warhead including the cumulative number of fragments versus fragment mass, fragment number distribution versus Θ, and fragment velocities versus Θ had been modeled with the CALE-PAFRAG code. Results of these analyses are shown in Figs. 4 and 5.

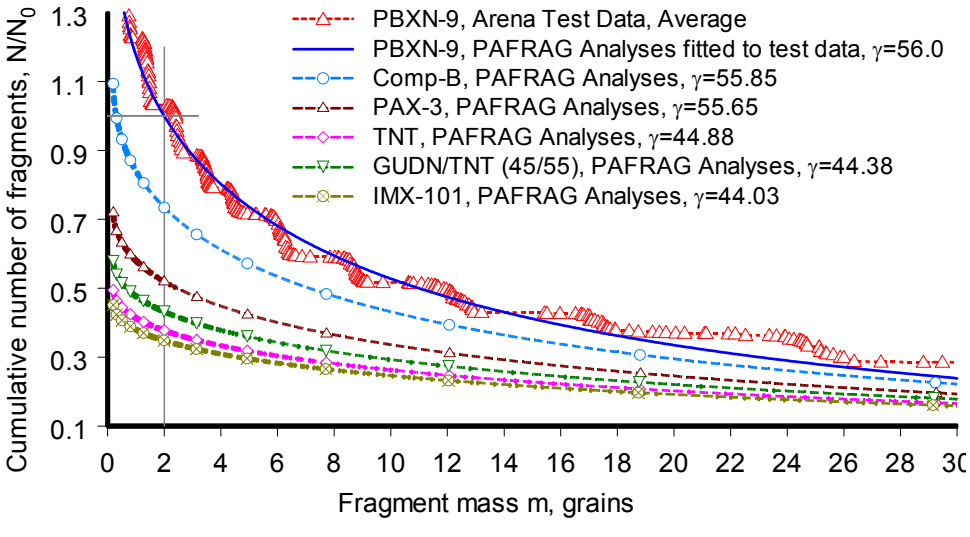

Fig. 4 Cumulative number of fragments versus fragment mass, Charge B

Fig. 4 shows a plot of a family of curves representing cumulative number of fragments of the prototype "Charge B" warhead for the PBXN-9, the Comp-B, the PAX-3, the TNT, the GUDN/TNT (45/55), and the IMX-101 explosive formulations. All detonation parameters for these explosive compositions including the Chapman-Jouguet detonation pressures had been calculated through thermochemical equilibrium analyses using the JAGUAR code [12]. The thermochemical models for the PBXN-9, the Comp-B, and the PAX-3 explosive formulations had been correlated with the available cylinder test, detonation velocity, and the detonation dent plate data; the analyses for the IMX-101 formulation had been correlated only with cylinder test data; the analyses for the GUDN/TNT (45/55) composition had been correlated with the cylinder test and the detonation velocity data for the pure GUDN explosive. As shown in the figure, PAFRAG code predictions of the decreases of the cumulative number of fragments are in a good agreement with the decreases of the Chapman-Jouguet detonation pressures and the explosive detonation energy calculated from the JAGUAR code.

Fig. 5 shows CALE-PAFRAG code predictions of the fragment velocities versus the fragment spray angle Θ. Since in an explosive fragmentation munition the

fragmenting shell accelerates through a series of the stress wave "pushes" and "pulls", significant through-thickness radial velocity gradients are present throughout all phases of shell dilation until it raptures generating a "spray" of fragments moving through the air. The scattered "dot-like" data points shown in the plot represent velocities of individual computational cells that can be compared with the velocities of individual fragments comprising the resulting fragment "spray cloud". As shown in the figure, the PAFRAG fragment velocity predictions are in a good agreement with the baseline PBXN-9 warhead arena test data representing velocities of the leading fringe of the fragment spray that reach the velocity measuring screens first. The solid curves shown in the plot represent the "momentum averaged" Θ-zone velocities, that is the total momentum of fragments in the Θ-zone divided over the mass of fragments in that zone. As shown in the figure, PAFRAG code predictions of the decreases of the momentum average Θ-zone velocities are in a good agreement with the decreases of the explosive detonation energy calculated from the JAGUAR code.

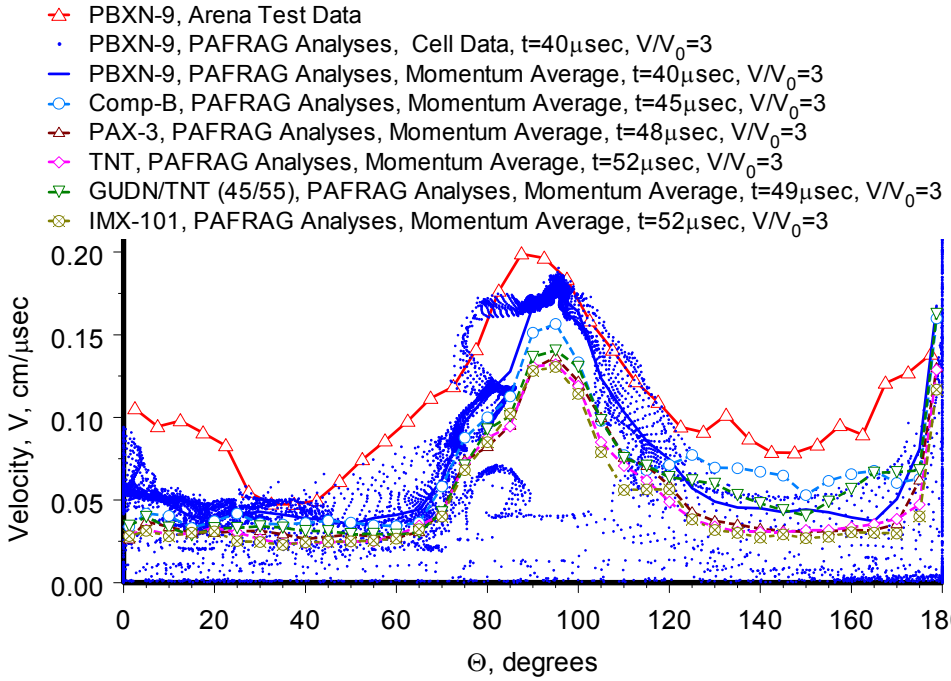

Fig. 5 Fragment velocities versus Θ for varying explosive compositions, Charge B

5. Acknowledgements.

Dr. E. L. Baker and Messrs. L. Sotsky, A. J. Mock, and P. J. Samuels of US Army ARDEC are acknowledged for providing initiative, support and funds that made this work possible. Professor L. I. Stiel of Polytechnic Institute of New York University is acknowledged for his contributions in thermochemical equilibrium modeling. Mr. W. Ramos of US Army ARDEC is acknowledged for his contribution in CALE modeling. Messrs. T. Wu and W. J. Poulos of US Army ARDEC are acknowledged for their contributions in directing sawdust fragmentation experimentation.

References

[1] V. M. Gold, "An Engineering Model for Design of Explosive Fragmentation Munitions (U)", Technical Report ARAET-TR-07001, Picatinny Arsenal, New Jersey, February 2007.

[2] R. E. Tipton, "CALE users manual", Version 910201, Lawrence Livermore National Laboratory, 1991.

[3] V. M. Gold, E. L. Baker, W. J. Poulos, and B. E. Fuchs, "PAFRAG Modeling of Performance of Explosive Fragmentation Munitions", Int. J. Imp. Engng., Vol. 33, pp. 294-304, 2006.

[4] N. F. Mott, F.R.S., "Fragmentation of steel cases", Proc. Roy. Soc., Vol. 189, pp. 300-308, 1947.

[5] D. E. Grady, "Fragmentation of Ring and Shells. The legacy of N. F. Mott", Springer-Verlag, New York, 2006.

[6] N. F. Mott and E. H. Linfoot, "A theory of fragmentation", Ministry of Supply, A.C. 3348, January 1943.

[7] N. F. Mott, "A theory of fragmentation of shells and bombs", Ministry of Supply, A. C. 4035, May 1943.

[8] D. E. Grady, "Natural fragmentation of conventional warheads", Sandia Report No. SAND90-0254, Sandia National Laboratory, Albuquerque, New Mexico, May 1990.

[9] Picatinny Arsenal Manual No. 5-1, "Testing Manual, Subject: Fragmentation Testing Procedures", Picatinny Arsenal, New Jersey, 24 August 1950.

[10] D. J. Steinberg, S. G. Cochran, and M. W. Guinan, "A constitutive model for metals applicable at high-strain rate", J Appl. Phys. 51:1498–504, 1980.

[11] D. R. Curran, L. Seaman, and D. A. Shockey, "Linking Dynamic Fracture to Microstructural Processes", in "Shock Waves and High-Strain-Rate Phenomena in Metals" (eds. M. A. Meyers and L. E. Murr), pp. 129-167, Plenum Press, New York, 1981.

[12] L. I. Stiel, Polytechnic Institute of NYU, Private communications, 2008.